AAC Journals.ASM.org

Differential CYP 2D6 Metabolism Alters Primaquine Pharmacokinetics

Brittney M. J. Potter,[a] Lisa H. Xie,[a] Chau Vuong,[a] Jing Zhang,[a] Ping Zhang,[a] Dehui Duan,[a] Thu-Lan T. Luong,[a] H. M. T. Bandara Herath,[b] N. P. Dhammika Nanayakkara,[b] Babu L. Tekwani,[b,c] Larry A. Walker,[b,c] Christina K. Nolan,[a] Richard J. Sciotti,[a] Victor E. Zottig,[a] Philip L. Smith,[a] Robert M. Paris,[a] Lisa T. Read,[a] Qigui Li,[a] Brandon S. Pybus,[a] Jason C. Sousa,[a] Gregory A. Reichard,[a] Sean R. Marcsisin[a]

Military Malaria Research Program, Division of Experimental Therapeutics, Walter Reed Army Institute of Research, Silver Spring, Maryland, USA[a]; National Center for Natural Products Research[b] and Department of Pharmacology, School of Pharmacy,[c] University of Mississippi, Mississippi, USA

Primaquine (PQ) metabolism by the cytochrome P450 (CYP) 2D family of enzymes is required for antimalarial activity in both humans (2D6) and mice (2D). Human CYP 2D6 is highly polymorphic, and decreased CYP 2D6 enzyme activity has been linked to decreased PQ antimalarial activity. Despite the importance of CYP 2D metabolism in PQ efficacy, the exact role that these enzymes play in PQ metabolism and pharmacokinetics has not been extensively studied *in vivo*. In this study, a series of PQ pharmacokinetic experiments were conducted in mice with differential CYP 2D metabolism characteristics, including wild-type (WT), CYP 2D knockout (KO), and humanized CYP 2D6 (KO/knock-in [KO/KI]) mice. Plasma and liver pharmacokinetic profiles from a single PQ dose (20 mg/kg of body weight) differed significantly among the strains for PQ and carboxy-PQ. Additionally, due to the suspected role of phenolic metabolites in PQ efficacy, these were probed using reference standards. Levels of phenolic metabolites were highest in mice capable of metabolizing CYP 2D6 substrates (WT and KO/KI 2D6 mice). PQ phenolic metabolites were present in different quantities in the two strains, illustrating species-specific differences in PQ metabolism between the human and mouse enzymes. Taking the data together, this report furthers understanding of PQ pharmacokinetics in the context of differential CYP 2D metabolism and has important implications for PQ administration in humans with different levels of CYP 2D6 enzyme activity.

Primaquine (PQ) is the only FDA-approved drug for treatment of relapsing infections with malarial strains, including *Plasmodium vivax* and *P. ovale* (1–3). PQ belongs to the 8-aminoquinoline (8AQ) class of antimalarial compounds, among which several molecules, including PQ, have potent antihypnozoite activity (2, 4, 5). Low doses of PQ are also recommended for malaria transmission-blocking efforts due to PQ's gametocidal activity (6, 7). PQ's utility in malaria treatment and potential use in malarial transmission reduction and malaria eradication efforts require an understanding of the molecular species involved in its mechanism of action.

Recent reports have shown that PQ requires metabolic activation by the cytochrome P450 (CYP) 2D isoenzymes for liver-stage antimalarial activity in both mouse studies (CYP 2D) and human studies (CYP 2D6) (8–11). Pybus et al. demonstrated that PQ was active only in mice capable of metabolizing CYP 2D6 substrates. Deletion of the mouse enzyme closest to human CYP 2D6 (mouse CYP 2D22 via deletion of the CYP 2D gene cluster) in mice completely blocked liver-stage antimalarial activity *in vivo* (10). The study by Bennett et al. demonstrated a direct link between CYP 2D6 metabolizer status and PQ efficacy for *P. vivax* treatment in several human subjects (8). PQ therapy is of significant importance for *P. vivax* radical cure, presumptive antirelapse therapy (PART), and malaria eradication efforts, and the requirement of CYP 2D6 metabolism for PQ efficacy is problematic because CYP 2D6 is highly polymorphic in human populations. Human CYP2D6 activity is highly variable, and more than 74 CYP 2D6 alleles have been reported to date (see references 12, 13, 14, and 15 for reviews on CYP 2D6 and metabolizer status). CYP 2D6 genetic and phenotypic differences can contribute to substantial differences in the metabolism and pharmacokinetics (PK) of CYP 2D6 substrates. There is limited information on the metabolic and pharmacokinetic consequences associated with differential CYP 2D6 metabolism status for PQ.

We sought to extend our previous studies of CYP 2D6 involvement with PQ activation (10, 11) by determining the pharmacokinetic consequences of differential CYP 2D metabolism for PQ and several of its metabolites. PQ is extensively metabolized both *in vitro* in the presence of hepatic microsomes and *in vivo* (8–11, 16–18). The predominant and most thoroughly studied metabolite of PQ is the carboxyl form, carboxyprimaquine (CPQ) (19). PQ also is extensively hydroxylated on the quinoline core (11, 16, 17, 20). The hydroxylated metabolites of PQ at positions 2, 3, and 4 were prepared synthetically as reference standards (see Fasinu et al. [20]). These reference standards (illustrated in Fig. 1) were utilized to probe these positions for *in vivo* hydroxylation. 5-Hydroxy primaquine is unstable with respect to both oxygen and light and is reported to auto-oxidize to a reactive 5,8 quinone-

Received 6 January 2015 **Returned for modification** 21 January 2015
Accepted 30 January 2015
Accepted manuscript posted online 2 February 2015
Citation Potter BMJ, Xie LH, Vuong C, Zhang J, Zhang P, Duan D, Luong T-LT, Bandara Herath HMT, Dhammika Nanayakkara NP, Tekwani BL, Walker LA, Nolan CK, Sciotti RJ, Zottig VE, Smith PL, Paris RM, Read LT, Li Q, Pybus BS, Sousa JC, Reichard GA, Marcsisin SR. 2015. Differential CYP 2D6 metabolism alters primaquine pharmacokinetics. Antimicrob Agents Chemother 59:2380–2387. doi:10.1128/AAC.00015-15.

Address correspondence to Sean R. Marcsisin, sean.r.marcsisin.mil@mail.mil.
B.M.J.P. and L.H.X. contributed equally to the article.

Supplemental material for this article may be found at http://dx.doi.org/10.1128/AAC.00015-15.

doi:10.1128/AAC.00015-15

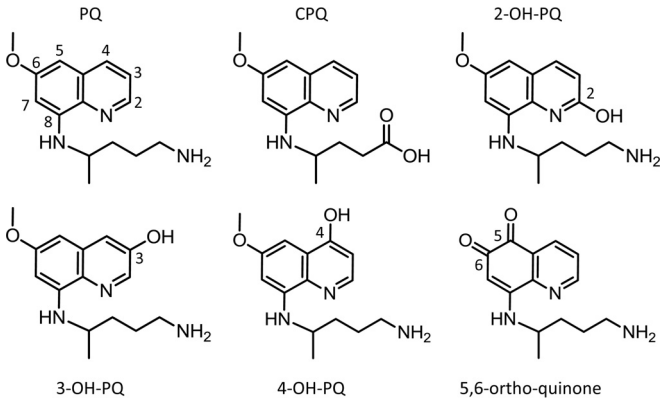

FIG 1 Compounds utilized in primaquine pharmacokinetic study. The structures of primaquine (PQ), carboxy-primaquine (CPQ), and 2, 3, and 4 hydroxylated primaquine (OH-PQ) are shown. The marker for 5-hydroxylation (5,6-ortho-quinone) is also shown. The quinoline rings of PQ and the hydroxylated metabolites are numbered for reference.

imine (21) capable of redox cycling. We found that the auto-oxidation cascade of 5-OH PQ terminates in a chemically stable 5,6-ortho-quinone species in the presence of oxygen and water (see the supplemental material). The 5,6-ortho-quinone is a tautomer of the 6-hydroxy, 5,8-quinone imine of PQ; however, nuclear magnetic resonance (NMR) analysis indicated that this metabolite likely exists in the 5,6-ortho-quinone form. This 5,6-ortho-quinone species was therefore utilized as a surrogate standard for species in the 5-hydroxylation pathway. Phenolic hydroxylation at position 5 is the proposed metabolic activation event required to produce unstable reactive metabolites capable of redox cycling. These redox cycling metabolites are the putative species thought to be responsible for the hemolytic toxicity and, likely, the antimalarial efficacy of PQ (10, 11, 16, 17, 21, 22).

The analytical standards shown in Fig. 1 were utilized to profile PQ pharmacokinetics in mice with differential levels of CYP 2D metabolism. Wild-type (WT) C57BL/6 mice (extensive metabolizers [EM]), CYP_{mouse} 2D knockout (KO) mice (poor metabolizers [PM]), and KO/CYP_{human} 2D6 knock-in (KO/KI) mice were selected for this study. PQ has been found to be most active against *Plasmodium berghei* in the WT mice (10), which express the CYP 2D22 enzyme, the nearest murine ortholog to human CYP 2D6 (23). PQ is inactive in mice lacking the CYP 2D22 enzyme (deletion of the CYP 2D gene cassette; see reference 24 for strain description) (10). Pharmacokinetic comparison of PQ in the WT versus KO mice was predicted to provide insight into pharmacokinetic differences for PQ and PQ metabolites in the mouse EM and PM phenotypes. Additionally, the CYP_{mouse} 2D knockout KO/CYP_{human} 2D6 knock-in (KO/KI) strain was utilized, as this strain expresses human CYP 2D6 instead of CYP 2D22, providing an opportunity to explore the metabolic differences in PQ metabolism between the mouse and human 2D isoforms.

MATERIALS AND METHODS

Abbreviations. 8AQ, 8-aminoquinoline; CYP, cytochrome P450; PQ, primaquine; CPQ, carboxyprimaquine; 2-OH-PQ, 2-hydroxy-primaquine; 3-OH-PQ, 3-hydroxy-primaquine; 4-OH-PQ, 4-hydroxy-primaquine; 5-OH-PQ, 5-hydroxy-primaquine; WT, wild type; KO, CYP 2D knockout; KO/KI, CYP 2D knockout/CYP 2D6 knock-in.

Pharmacokinetic measurements. Male 6-to-14-week-old C57BL/6 and 2D knockout and 2D knockout/2D6 knock-in C57BL/6 mice (Taconic, Hudson, NY) were used for PK evaluations. On arrival, animals were acclimated for 7 days in quarantine. The animals were housed in a cage maintained at a temperature range of 64 to 79°F and a relative humidity range of 34% to 68% with a 12-h light/dark cycle. Food and water were provided *ad libitum* during quarantine and throughout the study. The animals were fed a standard rodent maintenance diet. All animal studies were performed under IACUC-approved protocols. These protocols detail the experimental procedures and designs as well as number of animals used. The research was conducted in compliance with the Animal Welfare Act and other federal statutes and regulations relating to animals and experiments involving animals and adheres to principles stated in the *Guide for the Care and Use of Laboratory Animals* (28).

PK studies were performed using oral administration. For each time point (0, 0.5, 1, 2, 4, 6, 8, and 24 h), three male mice of each corresponding group were dosed with PQ (20 mg/kg of body weight). PQ was reconstituted in double-distilled water (ddH_2O) and administered at 100 μl/20 g. For each time point, whole-blood and -liver samples were collected. Plasma was obtained from whole blood (500 μl) collected by cardiac puncture. Heparin (Hospira, Lake Forest, IL) (500 μl of 1,000 USP U/ml) was added to whole-blood samples to prevent coagulation prior to plasma isolation via centrifugation. Isolated plasma samples were stored at −80°C until liquid chromatography-tandem mass spectrometry (LC-MS/MS) analysis. Liver samples were extracted for each time point and immediately preserved on dry ice and stored at −80°C until homogenization, extraction, and LC-MS/MS analysis.

LC-MS/MS analysis. All samples were analyzed using a Waters TQ MS mass spectrometer (Waters, Milford, MA, USA). Chromatographic separations were achieved using a Waters XTerra MS C_{18} analytical column (50 mm by 2.1 mm; 3-μm inner diameter [i.d.]), a Waters I class liquid chromatography system flowing at 0.40 ml/min, and a 6-min linear gradient from 5% to 98% acetonitrile (0.1% formic acid). The samples (10 μl each) were detected with electrospray ionization in the positive ion mode. Mass spectrometry conditions were optimized for PQ, CPQ, 2-hydroxy-primaquine (2-OH-PQ), 3-hydroxy-primaquine (3-OH-PQ), 4-hydroxy-primaquine (4-OH-PQ), and the 5,6-o-quinone (see the supplemental material for the reference retention times and MS/MS fragments monitored). Peak areas for PQ, CPQ, 2-OH-PQ, 3-OH-PQ, 4-OH-PQ, and the 5,6-o-quinone were extracted using Waters Mass Lynx software. The PQ, CPQ, 2-OH-PQ, 3-OH-PQ, 4-OH-PQ, and the 5,6-o-quinone plasma standard curves (0.5 to 1,000 ng/ml) and quality control samples were prepared by spiking blank mouse plasma and serially diluting to the desired concentration. The PQ, CPQ, 2-OH-PQ, 3-OH-PQ, 4-OH-PQ, and the 5,6-o-quinone liver standard curves (0.5 to 1,000 ng/ml) and quality control samples were prepared by spiking blank liver homogenate and serially diluting to the desired concentration. All standard curves, quality control samples, and PK samples were prepared for analysis by extraction with two volumes of acetonitrile with an internal standard (mefloquine) for each volume of sample. Liver samples were diluted with 5 volumes of water (1 ml/gram of liver) and homogenized prior to extraction. Each sample was subjected to vortex mixing and centrifuged at 16,000 × *g* for 10 min at 4°C. The supernatant was transferred to a 96-well plate for LC-MS/MS analysis. Compound concentrations were interpolated from each corresponding standard curve. Samples with LC-MS signal responses greater than the response from each corresponding standard curve (0.5 to 1,000 ng/ml) were diluted and reanalyzed for concentration determinations.

PK parameter determination. Pharmacokinetic parameters for PQ, carboxy-PQ, and the different phenolic metabolites in plasma and liver were determined using noncompartmental analysis via the Phoenix-WinNonlin software package (version 6.3; Pharsight Corp., Mountain View, CA). The maximum plasma concentration (C_{max}) and the time to maximum concentration (t_{max}) were directly obtained from the plasma and liver drug concentration-time curves. The elimination half-life ($t_{1/2}$) was calculated from $\ln 2/k_{el}$, which is the elimination rate constant calculated from the concentration-time plot. The area under the concentration-time

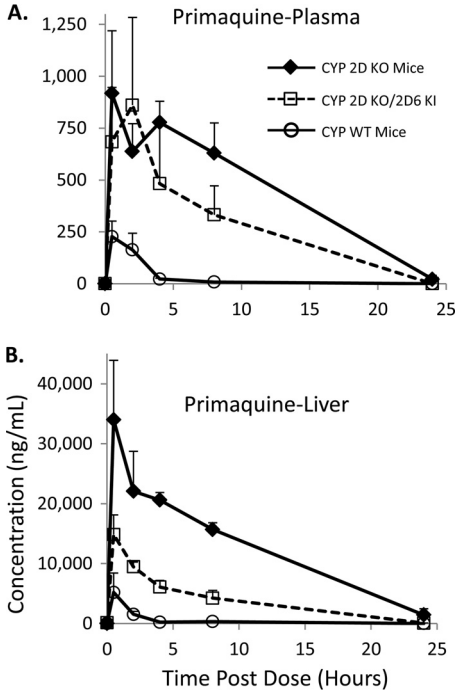

FIG 2 Pharmacokinetic profiles of primaquine. (A) Primaquine (PQ) pharmacokinetics in plasma from the various mouse strains tested. (B) PQ pharmacokinetics in liver from the various mouse strains tested. Concentrations shown are in ng/ml. The error shown for each measurement is the standard deviation from triplicate analyses. Three animals were utilized for each time point.

curve (AUC) was determined by the linear trapezoidal rule with extrapolation to infinity based on the concentration of the last time point divided by the terminal rate constant. The apparent clearance rate (CL) was determined by dividing the dose by the AUC from time zero to infinity (AUC_{INF}). Mean residence time (MRT) was determined by dividing the area under the first moment curve (AUMC) by AUC. Relative total systemic clearance (CL/F_obs) and the apparent volume of distribution during the steady state (V_Z/F_obs) were also estimated from the noncompartmental analysis. Pharmacokinetic parameter differences were compared for statistical significance determinations using a Welch's *t* test.

RESULTS

Pharmacokinetics of primaquine. The pharmacokinetic profiles of PQ were assessed in the WT, KO, and KO/KI mice after a single oral dose of 20 mg/kg. Pharmacokinetic samples were collected at up to 24 h post-PQ administration. The pharmacokinetic profiles of PQ in the WT mice, KO/KI mice, and KO mice are shown in Fig. 2. Figure 2A shows PQ plasma pharmacokinetics, while Fig. 2B shows liver pharmacokinetics. For both matrices, levels of PQ were highest in the KO mice. PQ has no antimalarial activity in the KO mice (10), and the pharmacokinetic results shown in Fig. 2 demonstrate that CYP 2D deficiency decreases PQ clearance and likely prevents metabolism of PQ to the presumed active metabolite(s) or at least significantly alters the kinetics of their release. The profile for the KO/KI mice indicates that initial PQ levels were similar to those seen with the KO mice; however, PQ levels were lower from h 4 to h 24, indicating increased PQ clearance compared to the KO strain. PQ is most efficacious in WT C57BL/6 mice (10), and PQ levels were lowest in this strain.

The pharmacokinetic parameters from the profiles shown in Fig. 2 were calculated using standard noncompartmental analysis for further comparison of PQ pharmacokinetics in the various mouse strains. Table 1 contains all the pharmacokinetic parameters determined for PQ in the various mice, including all the PQ plasma parameters in WT, KO/KI, and KO mice. Additionally, the *P* values for each parameter for the KO/KI and KO mice were determined by comparison to the WT pharmacokinetic parameters. The parent PQ exposure was lowest in the WT strain, as

TABLE 1 Pharmacokinetic parameters of primaquine tested in mice[a]

Primaquine parameter	Value(s)				
	WT mice ($n = 3$)	CYP 2D KO/2D6 KI mice ($n = 3$)	*P* value (WT vs KO/KI)	CYP 2D KO mice ($n = 3$)	*P* value (WT vs KO)
Plasma					
$T_{1/2}$ (h)	1.5 ± 0.4	3.9 ± 1.9	0.2	3.5 ± 0.9	0.04
T_{max} (h)	1.0 ± 0.9	2.2 ± 1.8	0.4	1.6 ± 2.0	0.6
C_{max} (ng/ml)	249.0 ± 37.0	1,001.3 ± 204.6	0.01	1,017.0 ± 139.9	0.006
$AUC_{0\text{-last}}$ (h · ng/ml)	596.8 ± 119.2	4,302.5 ± 319.9	0.0003	10,874.3 ± 1,470.7	0.007
$AUC_{0\text{-inf}}$ (h · ng/ml)	615.8 ± 112.9	6,453.5 ± 2,248.2	0.05	10,999.8 ± 1,342.6	0.006
V_Z/F (ml/kg)	73,395.1 ± 24,949.1	17,237.8 ± 2,950.5	0.6	9,601.8 ± 3,673.3	0.05
CL/*F* (ml/h/kg)	33,259.2 ± 6,439.1	3,324.5 ± 972.1	0.02	1,836.7 ± 227.8	0.01
$MRT_{0\text{-last}}$ (h)	1.81 ± 0.3	3.4 ± 0.5	0.02	6.1 ± 0.3	0.00004
Liver					
$T_{1/2}$ (h)	3.6 ± 1.2	2.9 ± 0.2	0.5	5.0 ± 1.5	0.3
T_{max} (h)	0.5 ± 0	0.5 ± 0	NA	0.5 ± 0	NA
C_{max} (ng/ml)	4,915.5 ± 3,068.9	14,064.7 ± 3,078.4	0.02	32,184.7 ± 9,347.1	0.041
$AUC_{0\text{-last}}$ (h · ng/ml)	8,683.8 ± 3,749.8	87,629.9 ± 7,742.6	0.0005	286,582.4 ± 19,777.2	0.002
$AUC_{0\text{-inf}}$ (h · ng/ml)	10,355.6 ± 4,284.5	87,873.1 ± 7,693.9	0.0006	297,827.5 ± 10,050.1	0.00002
V_Z/F (ml/kg)	11,346.7 ± 6,543.3	957.2 ± 145.6	0.1	488.2 ± 156.7	0.1
CL/*F* (ml/h/kg)	2,219.8 ± 1,068.9	228.8 ± 20.0	0.08	67.2 ± 2.2	0.08
$MRT_{0\text{-last}}$ (h)	1.8 ± 0.5	5.0 ± 0.6	0.002	6.2 ± 0.7	0.003

[a] Pharmacokinetic parameters from plasma and liver determinations are shown for the various mouse strains. Units for each parameter are indicated, and the errors shown are the standard deviations of the results from triplicate analyses. *P* values from comparisons of the KO and KO/KI strains to the WT C57BL/6 mice are also indicated. NA, not applicable; calculated values were identical and statistical analysis could not be performed.

reflected by the lowest C_{max}, AUC, $T_{1/2}$, and $MRT_{0\text{-last}}$ values. The calculated values for apparent clearance (CL/*F*) and apparent volume of distribution (V_Z/F) were highest in the WT strain, indicating that the WT mice were better able to metabolize, convert, and clear PQ than the other strains. The PQ parameters calculated from the KO/KI humanized mice indicated that replacement of the CYP 2D gene cluster with human CYP 2D6 altered PQ pharmacokinetics compared to the WT mice. The C_{max} and $MRT_{0\text{-last}}$ values in the humanized mice were higher than in the WT (C_{max} $P = 0.01$, $MRT_{0\text{-last}}$ $P = 0.02$) mice. The humanized mice also had significantly higher calculated AUC values ($AUC_{0\text{-last}}$ $P = 0.0003$, $AUC_{0\text{-inf}}$ $P = 0.05$). The apparent clearance was significantly lower in the humanized mice than in the WT mice (CL/*F* $P = 0.02$). The pharmacokinetic comparison of the humanized CYP 2D KO/KI mice described above illustrates clear differences in PQ metabolism and clearance in WT versus KO/KI mice.

The results for PQ pharmacokinetics in the KO mice indicated even greater differences in PK parameters compared to the WT strain. CYP 2D deficiency increased $T_{1/2}$ (*P* value = 0.04), C_{max} (*P* value = 0.006), AUC ($AUC_{0\text{-last}}$ *P* value = 0.007, AUC_{INF} *P* value = 0.006), and $MRT_{0\text{-last}}$ (*P* value = 0.00004) values compared to the WT strain results. The apparent clearance and relative volume of distribution were significantly lower in the KO mice than in the WT mice (CL/*F* $P = 0.01$, V_Z/F $P = 0.05$).

The changes in PQ pharmacokinetics were also determined in mouse liver. Liver is the target tissue for PQ antihypnozoite activity. Liver results are shown in Table 1. Similarly to the plasma pharmacokinetics, differential CYP 2D metabolism in the humanized KO/KI and CYP 2D KO mice resulted in higher $MRT_{0\text{-last}}$ and $T_{1/2}$ values, higher AUC and C_{max} values, and decreased apparent clearance and relative bioavailability of parent PQ. The liver results are consistent with the plasma pharmacokinetics and illustrate that CYP 2D metabolism has a significant effect on PQ distribution and clearance in mice.

Pharmacokinetics of carboxy-primaquine. Carboxy-primaquine (CPQ) is a well-characterized major metabolite of PQ formed via the monoamine oxidase pathway (11). CPQ concentrations in the various mouse strains were monitored to determine if differential CYP 2D metabolism would alter CPQ levels *in vivo*. CPQ PK results in the various mouse strains are shown in Fig. 3. Plasma CPQ pharmacokinetic profiles are shown in Fig. 3A and illustrate that CPQ levels were highest in the CYP 2D KO mice followed by the humanized KO/KI mice and that the WT mice had the lowest levels. There were measurable levels of CPQ in the KO strain throughout the duration of the experiment; however, CPQ was not detectable after 24 h postdose in the WT and KO/KI mice. Similar trends were observed in mouse liver, as shown in Fig. 3B. The CPQ results in the various matrices also correspond to parent PQ levels. The higher concentrations of PQ as a result of decreased CYP 2D metabolism resulted in more PQ conversion to CPQ. The results in the various mouse strains illustrate a potential difference between human and mouse PQ pharmacokinetics, as CPQ levels from humans with differential CYP 2D6 status were not significantly different (8); however, the sample size in the clinical trial was limited.

Pharmacokinetics of primaquine phenolic metabolites. PQ undergoes various oxidations on the quinoline core which are mediated by CYP 2D6 (10, 11). Phenolic oxidation is thought to be responsible for the antimalarial activity and hemolytic toxicity associated with PQ therapy (10, 22). To determine the role of CYP 2D metabolism in relation to production of phenolic PQ metabolites *in vivo*, reference standards for 2-OH-PQ, 3-OH-PQ, and 4-OH-PQ were utilized for quantification (see Fig. 1). Additionally, the 5,6-ortho-quinone of PQ was utilized as a marker for 5-hydroxy-primaquine (5-OH-PQ), as preparations of 5-OH-PQ in our hands readily oxidize to the stable 5,6-ortho-quinone (see the supplemental material), which has also been reported as a product of PQ metabolism by other groups (17, 25). These reference standards were employed to quantitate concentrations of the various metabolites. Plasma pharmacokinetic results for the PQ phenolic metabolites in the various mouse strains are shown in Fig. 4. Each metabolite is indicated, and the concentrations in the various strains are shown. The results in panel i of Fig. 4A show that the 5-OH-PQ marker was not detectable in the KO mice. The 5-OH-PQ marker was detectable in the humanized KO/KI strain (Fig. 4A, panel ii) and reached a C_{max} of 72.5 ng/ml. The concentration of the 5-OH-PQ marker was highest in the WT strain (Fig. 4A, panel iii), reaching a C_{max} of 1,091.0 ng/ml.

Concentrations of the 4, 3, and 2 hydroxylated species are shown in Fig. 4B to D, respectively. Similarly to the 5-OH-PQ marker, there were no detectable levels of any hydroxylated species (panel i) in the KO strain, indicating that phenolic oxidation of PQ is primarily catalyzed by CYP 2D metabolism *in vivo*. There were detectable levels of the 4, 3, and 2 hydroxylated PQ in the KO/KI mice (panel ii). The 4-OH-PQ concentrations reached 341.6 ng/ml, the 3-OH-PQ concentrations 156.9 ng/ml, and the 2-OH-PQ concentrations 82.4 ng/ml. The results for the WT strain and the 4, 3, and 2 hydroxylated species in panel iii show that only the 4 and 2 hydroxylated species were detectable in

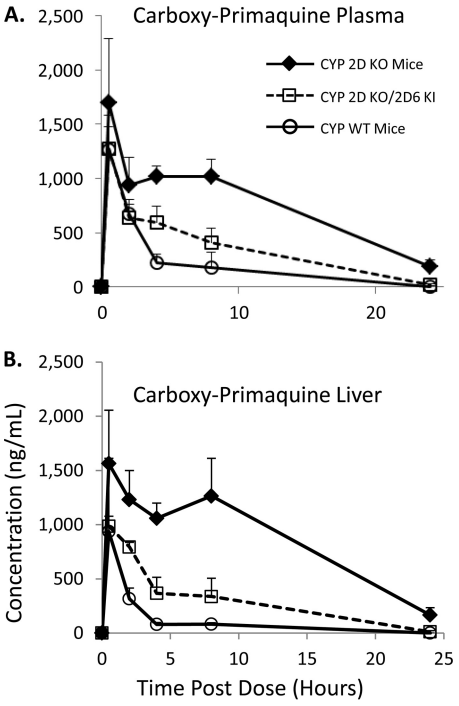

FIG 3 Pharmacokinetic profiles of carboxy-primaquine. (A) Carboxy-primaquine (CPQ) pharmacokinetics in plasma from the various mouse strains tested. (B) CPQ pharmacokinetics in liver from the various mouse strains tested. Concentrations shown are in ng/ml. The error shown for each measurement is the standard deviation from triplicate analyses. Three animals were utilized for each time point.

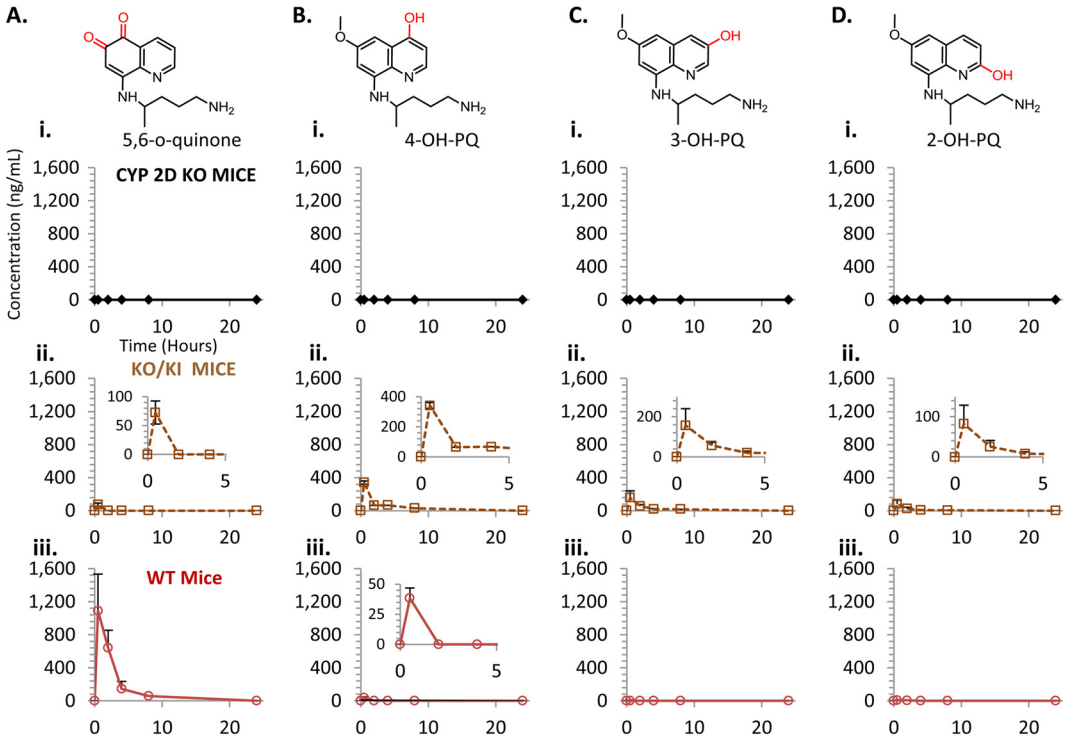

FIG 4 Plasma pharmacokinetic profiles of primaquine phenolic metabolites. (A) Pharmacokinetics of the 5,6-ortho-quinone of PQ in plasma from the various mouse strains tested. CYP 2D KO mice results are shown in panel i (diamonds, solid line), CYP 2D KO/2D6 KI mice are shown in panel ii (open squares, dashed line), and WT mice are shown in panel iii (open circles, solid line). (B) Pharmacokinetics of the 4-hydroxy-PQ in plasma. (C) Pharmacokinetics of the 3-hydroxy-PQ in plasma. (D) Pharmacokinetics of the 2-hydroxy-PQ in plasma. The various groups shown are the same as indicated above. Concentrations shown are in ng/ml. Insets are provided to magnify the metabolites present at lower levels. The error shown for each measurement is the standard deviation from triplicate analyses. Three animals were utilized for each time point.

plasma samples. The 4-OH-PQ concentrations reached 38.4 ng/ml, and the 2-OH-PQ concentrations reached 7.8 ng/ml.

Measurements of the PQ phenolic metabolites were also conducted in liver samples from the various mouse strains (Fig. 5). The pharmacokinetic trends for the phenolic species were similar to those obtained from plasma measurements. The results presented in panel i of Fig. 5A show that the 5-OH-PQ marker was detectable at only low levels in the KO mice (peak concentration of 535.3 ng/ml). The 5,6-ortho-quinone levels did not persist long enough in the KO mice for PK parameter determination. The 5-OH-PQ marker was detectable in the humanized KO/KI strain (Fig. 5A, panel ii) and reached a C_{max} of 2,189.5 ng/ml. The concentration of the 5-OH-PQ marker was highest in the WT strain (Fig. 5A, panel iii), reaching a C_{max} of 8,614.0 ng/ml. Concentrations of the 4, 3, and 2 hydroxylated species are shown in Fig. 5B, C, and D, respectively. There were only very low levels of these hydroxylated species (panel i) detected in the KO strain compared to the KO/KI and WT mice. Concentrations of these phenolic metabolites did not persist long enough in the KO mice for PK parameter determination. There were detectable levels of the 4, 3, and 2 hydroxylated PQ in the KO/KI mice (panel ii). The 4-OH-PQ concentrations reached 6,298.7 ng/ml, the 3-OH-PQ concentrations 6,486.1 ng/ml, and the 2-OH-PQ concentrations 1,126.9 ng/ml. The results for the WT strain and the 4, 3, and 2 hydroxylated species in panel iii show that the 4 hydroxylated species was detectable in liver samples. The 4-OH-PQ concentrations reached 1,093.5 ng/ml.

The calculated liver exposure values for the phenolic species are shown in Fig. 6. Liver exposure values reveal striking differences in the metabolites and the corresponding levels produced between the two strains. CYP 2D metabolism in the WT mice produced the 5,6-o-quinone preferentially over all other phenolic species. This is of interest because PQ is most efficacious in the WT strain and 5-OH-PQ has been suggested to be responsible for PQ's antimalarial activity and toxicity (10, 17, 22). The humanized KO/KI strain produced more 4-OH and 3-OH PQ than the other phenolic species. Exposure of the 5-OH-PQ marker in the humanized KO/KI mice was half that seen with the WT mice, and recent efficacy experiments have shown that 8AQ administration in the humanized KO/KI strain required approximately 2-fold dose escalation to achieve antimalarial activity comparable to that seen with the WT strain (26). The results determined for the various phenolic species also illustrate species-specific differences between the mouse CYP 2D and the human CYP 2D6 enzymes in PQ metabolism.

DISCUSSION

The work presented in this report demonstrates clear and significant differences in PQ pharmacokinetics in a mouse model of differential CYP 2D metabolism. Decreased metabolism and clearance via the CYP 2D pathway resulted in increased levels of exposure to parent PQ as well as to CPQ, a major metabolite produced via the monoamine oxidase pathway. Increased levels of PQ were also observed in humans with decreased CYP 2D6 activity (8). More significantly, 2D-deficient mice had significantly

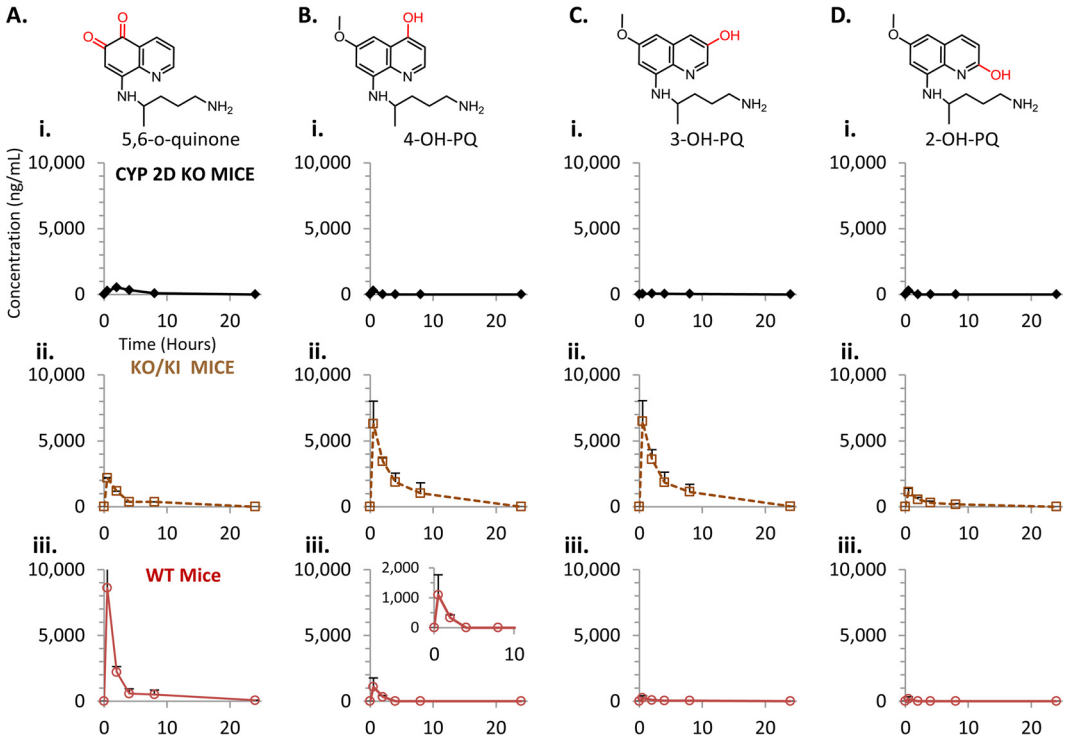

FIG 5 Liver pharmacokinetic profiles of primaquine phenolic metabolites. (A) Pharmacokinetics of the 5,6-ortho-quinone of PQ in liver from the various mouse strains tested. CYP 2D KO mice results are shown in panel i (diamonds, solid line), CYP 2D KO/2D6 KI mice are shown in panel ii (open squares, dashed line), and WT mice are shown in panel iii (open circles, solid line). (B) Pharmacokinetics of the 4-hydroxy-PQ in liver. (C) Pharmacokinetics of the 3-hydroxy-PQ in liver. (D) Pharmacokinetics of the 2-hydroxy-PQ in liver. The various groups shown are the same as indicated above. Concentrations shown are in ng/ml. Insets are provided to magnify the metabolites present at lower levels. The error shown for each measurement is the standard deviation from triplicate analyses. Three animals were utilized for each time point.

lower concentrations of phenolic metabolites, theorized to be integral for PQ efficacy, than the KO/KI and WT mouse strains. This phenomenon highlights the pharmacogenomic challenge of PQ administration for prophylaxis, *P. vivax* treatment, and/or malaria eradication efforts, since CYP 2D6 phenotypic nulls would likely show no cure and individuals with intermediate CYP 2D6 activity would potentially require higher PQ doses for successful *P. vivax* treatment. Additionally, decreased CYP 2D6 activity would result in higher systemic parent PQ concentrations. Elevated PQ concentrations could exacerbate toxicities and other unwanted side effects not normally observed in individuals with normal CYP 2D6 function generated by the parent drug (to exclude hemolytic toxicity, as this is likely linked with metabolic activation). Accumulation of parent 8AQ levels is more likely with 8AQ molecules (such as tafenoquine and NPC-1161B) with significantly longer half-lives than PQ; however, further investigation of these long half-life 8AQs is required to fully profile the effects of differential CYP 2D metabolism and 8AQ pharmacokinetics in both mice and humans.

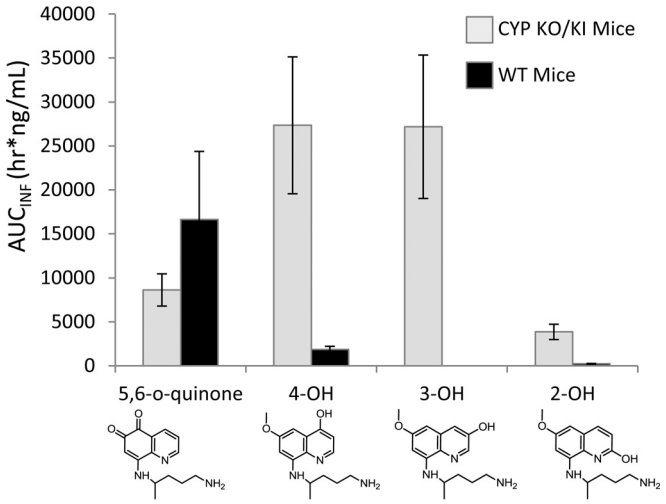

FIG 6 Liver exposure of primaquine phenolic metabolites in the KO/KI and WT mouse strains. Levels of liver exposure determined from AUC_{INF} (h · ng/ml) of 2-, 3-, 4-, and 5,6-o-quinone species of PQ are shown. Metabolites produced by the WT mice are indicated by black bars and metabolites produced by the KO/KI mice by gray bars. The error shown for each measurement is the standard deviation from triplicate analyses.

The pharmacokinetic results presented above for the PQ phenolic metabolites demonstrate clear differences in the types and quantities of PQ phenolic metabolites produced in WT and CYP 2D6 KI mice. This highlights differences in substrate metabolism between the mouse CYP 2D family of enzymes and human CYP 2D6. Mouse CYP 2D22 shares approximately 74% peptide sequence similarity with human CYP 2D6 and is likely the enzyme responsible for PQ metabolism in mice (23). Reports have indicated differences in substrate metabolism between the two enzymes (23, 24), and the results presented above indicate species-specific differences in PQ metabolism between the mouse CYP 2D enzymes and human CYP 2D6. Furthermore, our data suggest that, in mice, other CYPs in the 2D gene cluster may also play a role in PQ metabolism. The pharmacokinetics of PQ and the various metabolites in this study shows the utility of profiling 8AQ molecules for interspecies differences in CYP 2D metabolism. While the results presented above shed light on PQ metabolism in mice in the context of CYP 2D metabolism, additional clin-

ical studies are required to determine the relative pharmacokinetic/dynamic importance of each primaquine phenolic metabolite for PQ therapy in humans.

The 8AQ class of compounds demonstrates activity against various life cycle stages of the *Plasmodium* parasite (27). These include *Plasmodium* schizonts, hypnozoites, gameotocytes, and oocysts (27). These activities make the 8AQ class an attractive therapeutic class for malaria prophylaxis, treatment, and transmission-blocking efforts. The requirement of CYP 2D6 metabolism for 8AQ efficacy has been shown conclusively only for activity against the developmental liver stages of the *Plasmodium* parasite (8, 10, 26). Additional studies are required to determine if CYP 2D6 metabolism of PQ and other 8AQs is required for all observed antimalarial activity. Because *P. vivax* parasites currently cannot be cultured *in vitro* easily, and because the CYP 2D knockout approach is available only in a murine model, *P. berghei*-based *in vivo* models could serve as a viable surrogate for future studies exploring the role of CYP 2D6 metabolism for all observed 8AQ antimalarial activity. These studies could include investigations into PQ's gametocidal/transmission-blocking activity. Additionally, the gametocidal/transmission-blocking activity of primaquine could be directly assessed in human trials in individuals with known CYP 2D6 metabolizer status (i.e., poor, intermediate, and extensive CYP 2D6 metabolizers).

The pharmacokinetic information presented here, along with results from previous efficacy studies (8, 10), demonstrates that CYP 2D6 metabolism has a significant role in PQ pharmacokinetics and liver-stage antimalarial efficacy. PQ's CYP 2D6 pharmacogenomic liability should be considered by clinicians and policy makers for current and/or emerging PQ therapies, in the evaluation of patients who relapse after PQ therapy, and in the coprescription of drugs that are known CYP 2D6 inhibitors.

ACKNOWLEDGMENTS

We thank Liz Fitts and Anthony May of the Veterinary Services Branch, Walter Reed Army Institute of Research, for their assistance with acquisition of the various mouse strains utilized in this study. We also thank Jim McChesney and David Jollow for their scientific guidance and suggestions.

This work was supported in part by the Joint Warfighter Medical Research Program (JWMRP), award no. W81XWH1020059 and W81XWH1320026, and the Military Infectious Diseases Research Program (MIDRP), project no. Q0302_12_WR_CS.

This material has been reviewed by the Walter Reed Army Institute of Research. There is no objection to its presentation and/or publication. The opinions or assertions contained herein are the private views of the authors and are not to be construed as official or as reflecting true views of the Department of the Army or the Department of Defense.

We declare that we have no competing interests.

REFERENCES

1. **Coatney GR, Alving AS, Jones R, Jr, Hankey DD, Robinson DH, Garrison PL, Coker WG, Donovan WN, Di Lorenzo A, Marx RL, Simmons IH.** 1953. Korean vivax malaria. V. Cure of the infection by primaquine administered during long-term latency. Am J Trop Med Hyg **2:**985–988.
2. **Edgcomb JH, Arnold J, Yount EH, Jr, Alving AS, Eichelberger L, Jeffery GM, Eyles D, Young MD.** 1950. Primaquine, SN 13272, a new curative agent in vivax malaria; a preliminary report. J Natl Malar Soc **9:**285–292.
3. **Fernando D, Rodrigo C, Rajapakse S.** 2011. Primaquine in vivax malaria: an update and review on management issues. Malar J **10:**351. http://dx.doi.org/10.1186/1475-2875-10-351.
4. **Llanos-Cuentas A, Lacerda MV, Rueangweerayut R, Krudsood S, Gupta SK, Kochar SK, Arthur P, Chuenchom N, Mohrle JJ, Duparc S, Ugwuegbulam C, Kleim JP, Carter N, Green JA, Kellam L.** 2014. Tafenoquine plus chloroquine for the treatment and relapse prevention of Plasmodium vivax malaria (DETECTIVE): a multicentre, double-blind, randomised, phase 2b dose-selection study. Lancet **383:**1049–1058. http://dx.doi.org/10.1016/S0140-6736(13)62568-4.
5. **Price RN, Nosten F.** 2014. Single-dose radical cure of Plasmodium vivax: astepcloser.Lancet**383:**1020–1021.http://dx.doi.org/10.1016/S0140-6736(13)62672-0.
6. **Chotivanich K, Sattabongkot J, Udomsangpetch R, Looareesuwan S, Day NP, Coleman RE, White NJ.** 2006. Transmission-blocking activities of quinine, primaquine, and artesunate. Antimicrob Agents Chemother **50:**1927–1930. http://dx.doi.org/10.1128/AAC.01472-05.
7. **Eziefula AC, Gosling R, Hwang J, Hsiang MS, Bousema T, von Seidlein L, Drakeley C, Primaquine in Africa Discussion Group.** 2012. Rationale for short course primaquine in Africa to interrupt malaria transmission. Malar J **11:**360. http://dx.doi.org/10.1186/1475-2875-11-360.
8. **Bennett JW, Pybus BS, Yadava A, Tosh D, Sousa JC, McCarthy WF, Deye G, Melendez V, Ockenhouse CF.** 2013. Primaquine failure and cytochrome P-450 2D6 in Plasmodium vivax malaria. N Engl J Med **369:**1381–1382. http://dx.doi.org/10.1056/NEJMc1301936.
9. **Jin X, Pybus BS, Marcsisin SR, Logan T, Luong TL, Sousa J, Matlock N, Collazo V, Asher C, Carroll D, Olmeda R, Walker LA, Kozar MP, Melendez V.** 25 June 2013, posting date. An LC-MS based study of the metabolic profile of primaquine, an 8-aminoquinoline antiparasitic drug, with an in vitro primary human hepatocyte culture model. Eur J Drug Metab Pharmacokinet http://dx.doi.org/10.1007/s13318-013-0139-8.
10. **Pybus BS, Marcsisin SR, Jin X, Deye G, Sousa JC, Li Q, Caridha D, Zeng Q, Reichard GA, Ockenhouse C, Bennett J, Walker LA, Ohrt C, Melendez V.** 2013. The metabolism of primaquine to its active metabolite is dependent on CYP 2D6. Malar J **12:**212. http://dx.doi.org/10.1186/1475-2875-12-212.
11. **Pybus BS, Sousa JC, Jin X, Ferguson JA, Christian RE, Barnhart R, Vuong C, Sciotti RJ, Reichard GA, Kozar MP, Walker LA, Ohrt C, Melendez V.** 2012. CYP450 phenotyping and accurate mass identification of metabolites of the 8-aminoquinoline, anti-malarial drug primaquine. Malar J **11:**259. http://dx.doi.org/10.1186/1475-2875-11-259.
12. **Bernard S, Neville KA, Nguyen AT, Flockhart DA.** 2006. Interethnic differences in genetic polymorphisms of CYP2D6 in the U.S. population: clinical implications. Oncologist **11:**126–135. http://dx.doi.org/10.1634/theoncologist.11-2-126.
13. **Bogni A, Monshouwer M, Moscone A, Hidestrand M, Ingelman-Sundberg M, Hartung T, Coecke S.** 2005. Substrate specific metabolism by polymorphic cytochrome P450 2D6 alleles. Toxicol In Vitro **19:**621–629. http://dx.doi.org/10.1016/j.tiv.2005.04.001.
14. **Ingelman-Sundberg M.** 2005. Genetic polymorphisms of cytochrome P450 2D6 (CYP2D6): clinical consequences, evolutionary aspects and functional diversity. Pharmacogenomics J **5:**6–13. http://dx.doi.org/10.1038/sj.tpj.6500285.
15. **Zhou SF.** 2009. Polymorphism of human cytochrome P450 2D6 and its clinical significance: part I. Clin Pharmacokinet **48:**689–723. http://dx.doi.org/10.2165/11318030-000000000-00000.
16. **Vásquez-Vivar J, Augusto O.** 1992. Hydroxylated metabolites of the antimalarial drug primaquine. Oxidation and redox cycling. J Biol Chem **267:**6848–6854.
17. **Vásquez-Vivar J, Augusto O.** 1994. Oxidative activity of primaquine metabolites on rat erythrocytes in vitro and in vivo. Biochem Pharmacol **47:**309–316. http://dx.doi.org/10.1016/0006-2952(94)90022-1.
18. **Avula B, Tekwani BL, Chaurasiya ND, Nanayakkara NP, Wang YH, Khan SI, Adelli VR, Sahu R, Elsohly MA, McChesney JD, Khan IA, Walker LA.** 2013. Profiling primaquine metabolites in primary human hepatocytes using UHPLC-QTOF-MS with 13C stable isotope labeling. J Mass Spectrom **48:**276–285. http://dx.doi.org/10.1002/jms.3122.
19. **Mihaly GW, Ward SA, Edwards G, Orme ML, Breckenridge AM.** 1984. Pharmacokinetics of primaquine in man: identification of the carboxylic acid derivative as a major plasma metabolite. Br J Clin Pharmacol **17:**441–446. http://dx.doi.org/10.1111/j.1365-2125.1984.tb02369.x.
20. **Fasinu PS, Tekwani BL, Nanayakkara ND, Avula B, Herath HB, Wang YH, Adelli VR, Elsohly MA, Khan SI, Khan IA, Pybus BS, Marcsisin SR, Reichard GA, McChesney JD, Walker LA.** 2014. Enantioselective metabolism of primaquine by human CYP2D6. Malar J **13:**507. http://dx.doi.org/10.1186/1475-2875-13-507.
21. **Vasquez-Vivar J, Augusto O.** 1990. ESR detection of free radical inter-

mediates during autoxidation of 5-hydroxyprimaquine. Free Radic Res Commun **9:**383–389. http://dx.doi.org/10.3109/10715769009145698.
22. **Bowman ZS, Oatis JE, Jr, Whelan JL, Jollow DJ, McMillan DC.** 2004. Primaquine-induced hemolytic anemia: susceptibility of normal versus glutathione-depleted rat erythrocytes to 5-hydroxyprimaquine. J Pharmacol Exp Ther **309:**79–85. http://dx.doi.org/10.1124/jpet.103.062984.
23. **Yu AM, Haining RL.** 2006. Expression, purification, and characterization of mouse CYP2d22. Drug Metab Dispos **34:**1167–1174. http://dx.doi.org/10.1124/dmd.105.008870.
24. **Scheer N, Kapelyukh Y, McEwan J, Beuger V, Stanley LA, Rode A, Wolf CR.** 2012. Modeling human cytochrome P450 2D6 metabolism and drug-drug interaction by a novel panel of knockout and humanized mouse lines. Mol Pharmacol **81:**63–72. http://dx.doi.org/10.1124/mol.111.075192.
25. **Brossi A, Gessner W, Hufford CD, Baker JK, Homo F, Millet P, Landau I.** 1987. Photooxidation products of primaquine. Structure, antimalarial activity and hemolytic effects. FEBS Lett **223:**77–81.
26. **Marcsisin SR, Sousa JC, Reichard GA, Caridha D, Zeng Q, Roncal N, McNulty R, Careagabarja J, Sciotti RJ, Bennett JW, Zottig VE, Deye G, Li Q, Read L, Hickman M, Dhammika Nanayakkara NP, Walker LA, Smith B, Melendez V, Pybus BS.** 2014. Tafenoquine and NPC-1161B require CYP 2D metabolism for anti-malarial activity: implications for the 8-aminoquinoline class of anti-malarial compounds. Malar J **13:**2. http://dx.doi.org/10.1186/1475-2875-13-2.
27. **Delves M, Plouffe D, Scheurer C, Meister S, Wittlin S, Winzeler EA, Sinden RE, Leroy D.** 2012. The activities of current antimalarial drugs on the life cycle stages of Plasmodium: a comparative study with human and rodent parasites. PLoS Med **9:**e1001169. http://dx.doi.org/10.1371/journal.pmed.1001169.
28. **National Research Council.** 2011. Guide for the care and use of laboratory animals, 8th ed. National Academies Press, Washington, DC.